https://doi.org/10.5194/wes-2025-266
Preprint. Discussion started: 15 December 2025

eawe european academy of wind energy
Open Access WIND ENERGY SCIENCE DISCUSSIONS

Impacts of Climate Change on the Offshore Wind Industry in Metropolitan France: Insights from the 2C NOW Project

Youen Kervella[1], Tessa Chevallier[1], Boutheina Oueslati[2], Nicolas Raillard[3], Marissa Yates[6], Matéo Pimoult[7], Coline Poppeschi[1,3], Anindita Patra[1,2], Neil Luxcey[1], Florent Guinot[1], and Laurent Dubus[4,5]

[1]Wind and Ocean Dynamics department, France Energies Marines, Plouzané, France
[2]OSIRIS laboratory, EDF R&D, Palaiseau, France
[3]RDT, IFREMER, Plouzané, France
[4]Climate, Long-Term Power System Adequacy and Planning Group, RTE, Puteaux, France
[5]World Energy & Meteorology Council, Norwich, England
[6]LHSV, Ecole Nationale des Ponts et Chaussées, Chatou, France
[7]INNOSEA, OWC, ABL Group, Nantes, France

Correspondence: Youen Kervella (youen.kervella@france-energies-marines.org)

Abstract.

The offshore wind energy sector in France is poised for significant growth, with ambitious targets to install 18 GW of offshore capacity by 2035 and 45 GW by 2050. This expansion is crucial for achieving France's goal of generating 20% of its electricity from offshore wind by 2050. The 2C NOW project, led by France Energies Marines, investigates the impact of climate change on metocean conditions along France's three maritime fronts (two representative points for each seafront). This is critical in the context of sector development, which aims to support long-term energy transition goals and the sustainability of wind farms over several decades. Using global climate models from the CMIP6 project (IPCC), a statistical downscaling of the datasets is performed using the CDF-t method (Michelangeli et al., 2009) based on the best available numerical reanalyses (selected using extensive in-situ data). The mean conditions show a general decrease in wind speed and wave height (multi-model average) for all SSP scenarios and for all seafronts in continental France. This downward trend is more significant for the long-term future period (horizon 2100), on the Atlantic and Mediterranean coasts. These average trends are nevertheless accompanied by strong model uncertainties. Regarding extreme conditions, an increase in extreme values of significant wave height is observed for the future climate scenarios, while there is less consensus on the wind speed. Water levels show significant increasing trends, regardless of the seafront or the conditions concerned.

1 Introduction

Climate change is expected to profoundly reshape the environmental conditions which govern offshore wind energy production. In Europe, offshore wind is a cornerstone of the energy transition, with a target of 300 GW installed capacity by 2050 under the European Green Deal and REPowerEU strategies (European Commission, 2020; European Parliament, 2020). France, in

https://doi.org/10.5194/wes-2025-266
Preprint. Discussion started: 15 December 2025

eawe european academy of wind energy
Open Access WIND ENERGY SCIENCE DISCUSSIONS

particular, aims to reach 45 GW of offshore wind capacity by mid-century, making it essential to understand how climate-driven changes in metocean conditions may affect this trajectory.

Offshore wind offers several advantages over onshore wind, including higher and more consistent wind speeds, larger available areas, and reduced land-use conflicts. However, its performance and reliability are inherently sensitive to atmospheric and oceanic conditions, which are themselves subject to evolve in time due to climate change. Recent studies, like (Rapella et al., 2023), have shown that climate change is already affecting the availability of offshore wind power in Europe through changes in the frequency and intensity of extreme wind events. These events can disrupt turbine operation by exceeding cut-out thresholds or falling below cut-in speeds, leading to significant losses in energy production.

Wind speed trends in Europe show a general decline (over a historical period from in-situ data or numerical reanalyses), particularly in summer months, due to changes in atmospheric circulation and land-sea thermal contrasts—a phenomenon known as "global terrestrial stilling" (Zeng et al., 2019; Wu et al., 2018). CMIP6-based projections suggest a reduction in average wind speeds of up to 5% by 2050 and potentially 10–15% by 2100, with regional variability (Hahmann et al., 2022; Susini et al., 2022). These changes could significantly affect the energy yield and economic viability of offshore wind farms.

The wave climate is also undergoing changes. CMIP6 projections for the Mediterranean Sea indicate a general decrease in significant wave height and wave energy flux under high-emission scenarios (SSP5-8.5), with some localized increases in the eastern basin (Ibarra-Berastegui et al., 2025). In the Atlantic and Channel regions, projections show increased variability and a potential rise in extreme wave events, which could impact structural design and maintenance strategies (Meucci et al., 2023).

Sea level rise is among the most certain consequences of climate change. In France, recent national assessments anticipate a rise exceeding 60 cm by 2100 under a 3°C global warming scenario, with significant regional variability due to vertical land motion and ocean dynamics (Le Cozannet and Cazenave, 2024). This rise will increase exposure to coastal hazards and affect offshore infrastructure design, especially in shallow or nearshore zones.

These changes have direct implications for offshore wind farm design, operation, and financial viability. The Levelized Cost of Energy (LCOE) may be affected by reduced energy yield, increased downtime, and the need for more robust infrastructure to withstand evolving metocean conditions. Moreover, the spatial coherence of weather regimes associated with extreme wind events raises concerns about simultaneous outages across multiple sites, potentially challenging grid stability and energy supply security (Rapella et al., 2023).

In this context, the 2C NOW project[1], led by France Energies Marines, addresses these challenges by assessing the evolution of wind, wave, and water level conditions along France's three maritime fronts. Using a combination of in-situ observations, reanalysis datasets, and statistically downscaled CMIP6 projections, the project aims to quantify future changes and evaluate their implications for offshore wind energy production, infrastructure design, and long-term planning.

The first section of this paper is dedicated to the datasets and the main mathematical methods used during the project. The second section presents the main evolutions of wind, waves and water levels. These evolutions are studied for mean and extreme conditions. The next section is dedicated to offshore wind by studying the evolution of wind energy production and design conditions. The limitations identified in the project are outlined at the end of this study.

[1] https://www.france-energies-marines.org/en/projects/2c-now/

https://doi.org/10.5194/wes-2025-266
Preprint. Discussion started: 15 December 2025

eawe european academy of wind energy
Open Access WIND ENERGY SCIENCE DISCUSSIONS

2 Data and methods

The methodology adopted in this study integrates observational and modeling approaches to quantify climate-driven changes in metocean conditions and their implications for offshore wind. First, long-term in-situ measurements were compiled and quality-controlled to ensure robust reference datasets. These observations guided the selection of the most suitable reanalysis product for each French coastline. The chosen reanalysis then served as the baseline for statistical downscaling of global climate models (GCMs) at representative offshore locations. Downscaled time series were subsequently analyzed to derive trends in wind speed, significant wave height, and water level under different climate scenarios. Finally, these projected changes were assessed in terms of their potential impact on offshore wind energy production and design conditions.

2.1 Datasets

Tables 1 and 2 present, respectively, the in-situ measurements and reanalyses datasets used in this study. The in-situ measurements for each parameter (table 1) were analyzed: each raw observation exceeding the daily mean value by a factor of 2 times the daily standard deviation was removed as an outlier (Bentamy and Croize-Fillon, 2014) and a maximum of 33% missing values in each month was allowed to obtain consistent scores. Different reanalyses were compared to these measurements over the period 1995-2018, taking into account average and extreme conditions as well as seasonal and diurnal cycles, and inter-annual variability (Patra et al. (2025)). The selected reanalyses are presented in table 2.

Table 1. In-situ measurements

Parameter	Dataset	Provider	Number of stations per seafront (after QC)			URL
			Channel	Atlantic	Med. Sea	
Wind	SYNOP 10m	Météo-France	7	11	6	https://meteo.data.gouv.fr/datasets/6569b4473bedf2e7abad3b72
Waves	in situ TAC buoys	CMEMS[2]	3	5	4	https://marine.copernicus.eu/
Water Levels	RONIM network	SHOM[3]	7	11	7	http://refmar.shom.fr/fr/partenaires/producteurs-de-donnees/reseau-maregraphique-ronim

The GCMs used in this study are part of the Coupled Model Intercomparison Project Phase 6 (CMIP6) and are listed in tables 3 and 4. Regarding 10 m wind, 13 GCMs were used in this study (table 3), following a set of criteria such as model performance, daily data availability or the representation of the ensemble spread in terms of climate response (Michelangeli et al. 2023). The 10 m wind data is available from 1950 to 2014 for the historical period and from 2015 to 2100 for the future scenarios (SSP1-2.6, SSP4-4.5, SSP3-7.0 and SSP5-8.5), at a daily timescale, for each model. For waves, eight GCMs were used (table 4) based on the work of Meucci et al., 2024. The wave data is available from 1985 to 2014 for the historical period

https://doi.org/10.5194/wes-2025-266
Preprint. Discussion started: 15 December 2025

Table 2. Reanalysis datasets by seafront

Parameter	Seafront	Reanalysis	Provider	Period	Res.	URL
Wind	English Channel, Atlantic and Med. Sea	CERRA	Copernicus	1984–2021	5.5 km, 3 h	https://cds.climate.copernicus.eu/datasets/reanalysis-cerra-single-levels?tab=overview
Waves	English Channel and Atlantic	HYWAT	SHOM	1979–2022	UNST, 1 h	https://doi.org/10.17183/REJEUX_HYWAT
	Med. Sea	MED-WAV	CMEMS	1993–2024	1/24°, 1 h	https://doi.org/10.25423/cmcc/medsea_multiyear_wav_006_012
Water Levels	English Channel, Atlantic and Med. Sea	GTSM-ERA5	CDS	1979–2018	0.1°, 10 min	https://cds.climate.copernicus.eu/cdsapp#!/dataset/sis-water-level-change-timeseries-cmip6?tab=overview

and from 2071 to 2100 for the future scenarios (only SSP1-2.6 and SSP5-8.5), at a 3h temporal resolution, for each model. For water levels, five GCMs were used (table 4) from the work of Muis et al. 2022. The water level data is available from 1950 to 2014 for the historical period and from 2015 to 2050 for only one future scenario (SSP5-8.5), at a 10-minute temporal resolution (storm surges, mean sea level -MSL- being common to all models and on an annual basis), for each model.

2.2 Statistical downscaling on representative points

Local conditions are not accurately represented by Global Climate Models (GCMs) due to their coarse spatial resolution and the misrepresentation of key physical processes. To improve local accuracy, statistical downscaling is applied at six offshore locations in this study (table 5). These points are representative of the location of offshore wind farms on each French seafront. Several statistical downscaling approaches exist, either correcting mean values or adjusting the full distribution. In this study, the latter is adopted: the CDF-t (Cumulative Distribution Function transform) method (Michelangeli et al., 2009). This method corrects the whole distribution and aims to preserve trends due to climate change.

In this method, the authors assume that a mapping exists between the global and local Cumulative Distribution Functions (global corresponding to the GCM and local to the reanalysis) for the current period, which is defined by:

$$T(F_{m,h}(x)) = F_{o,h}(x) \Longleftrightarrow T(u) = F_{o,h}(F^{-1}_{m,h}(u)), \tag{1}$$

with $F_{m,h}(x)$ the CDF of a GCM and $F_{o,h}(x)$ the CDF of the reanalysis.

https://doi.org/10.5194/wes-2025-266
Preprint. Discussion started: 15 December 2025

eawe european academy of wind energy
Open Access WIND ENERGY SCIENCE DISCUSSIONS

Table 3. List of the climate models for the wind speed used in this study.

Model	Provider	Spatial Resolution	ECS (°C)	Reference
ACCESS-ESM1-5	CSIRO (Australia)	140 km	3.87	Ziehn et al. (2019c), DOI:10.22033/ESGF/CMIP6.2288
BCC-CSM2-MR	BCC (China)	100 km	3.04	Xin et al. (2018), DOI:10.22033/ESGF/CMIP6.1725
CESM2-WACCM	NCAR (USA)	100 km	4.75	Danabasoglu (2019s), DOI:10.22033/ESGF/CMIP6.10024
CMCC-CM2-SR5	CMCC (Italy)	100 km	3.52	Lovato and Peano (2020a), DOI:10.22033/ESGF/CMIP6.1362
EC-Earth3	EC-Earth-Consortium (Europe)	80 km	4.1	EC-Earth Consortium (2019a), DOI:10.22033/ESGF/CMIP6.181
FGOALS-g3	CAS (China)	190 km	2.88	Li (2019a), DOI:10.22033/ESGF/CMIP6.1783
GFDL-ESM4	NOAA (USA)	100 km	2.60	Krasting et al. (2018b), DOI:10.22033/ESGF/CMIP6.1407
IPSL-CM6A-LR	IPSL (France)	160 km	4.56	Boucher et al. (2018c), DOI:10.22033/ESGF/CMIP6.1534
MIROC-ES2L	MIROC (Japan)	250 km	2.68	Hajima et al. (2019a), DOI:10.22033/ESGF/CMIP6.902
MPI-ESM1-2-LR	MPI (Germany)	170 km	3.00	Wieners et al. (2019b), DOI:10.22033/ESGF/CMIP6.742
MRI-ESM2-0	MRI (Japan)	100 km	3.15	Yukimoto et al. (2019e), DOI:10.22033/ESGF/CMIP6.621
NorESM2-LM	NorESM (Norway)	190 km	2.54	Seland et al. (2019a), DOI:10.22033/ESGF/CMIP6.502
UKESM1-0-LL	NIMSKMA (Korea)	140 km	5.34	Shim et al. (2020b), DOI:10.22033/ESGF/CMIP6.2245

Moreover the authors assume that this mapping stays valid in the future. Thus, it is possible to estimate the CDF of the future local data through the transformation of the available data. The final equation, to correct the cumulative density of the future period of the GCM is given by:

$$F_{o,f}(x) = F_{o,h}(F^{-1}_{m,h}(F_{m,f}(x))), \tag{2}$$

with $F_{m,f}(x)$ the CDF of the future period of the GCM and $F_{o,f}(x)$ its corrected cumulative density.

An example of application of the CDF-t method is given in figure 1.

https://doi.org/10.5194/wes-2025-266
Preprint. Discussion started: 15 December 2025

eawe european academy of wind energy
Open Access WIND ENERGY SCIENCE DISCUSSIONS

Table 4. Wave and water level climate datasets used in this study.

Parameter	Dataset	Provider	Resolutions	Scenarios	Wind models	URL
Waves	8-model ensemble (Meucci et al.)	CSIRO	0.5°, 3 h	Historical (1985-2014), SSP1-2.6 (2071–2100), SSP5-8.5 (2071–2100)	ACCESS-CM2, AWI-CM-1-1-MR, CMCC-CM2-SR5, EC-Earth3, IPSL-CM6A-LR, KIOST-ESM, MPI-ESM1-2-LR, MRI-ESM2-0	https://polar.ncep.noaa.gov/waves
Water Levels	GTSM	CDS	0.1°, 10 min	Historical (1950–2014), SSP5-8.5 (2015–2050)	CMCC-CM2-VHR4, EC-Earth3P-HR, GFDL-CM4C192-SST, HadGEM3-GC31-HM, HadGEM3-GC31-HM-SST	https://cds.climate.copernicus.eu/datasets/sis-water-level-change-timeseries-cmip6?tab=overview

Table 5. Seafront representative points coordinates.

Name	Latitude (WGS84)	Longitude (WGS84)
EChan (Eastern Channel)	50.10	0.20
WChan (Western Channel)	49.20	-2.75
NAtl (Northern Atlantic)	47.45	-3.85
SAtl (Southern Atlantic)	45.60	-1.90
WMed (Western Mediterranean)	42.65	3.30
EMed (Eastern Mediterranean)	43.05	4.75

2.3 Extreme value analysis

For both design and operation & maintenance (O&M) purposes, developers are often interested in estimating severe to extreme environmental conditions. The study was focus on the modeling of extremes of 10 m wind speed, significant wave height and storm surges. Two main approaches are common in univariate extreme value modeling (see e.g. (Coles, 2001)), the Bloc Maxima (BM) method and the Peaks Over Threshold (POT) approach. The first one relies on modeling the maximal value obtained on disjoint blocs of the same size (usually, a year or a month) using a Generalized Extreme Value (GEV) distribution. The second one models every exceedance above a high, user-defined threshold (usually, a high quantile of the original data)

https://doi.org/10.5194/wes-2025-266
Preprint. Discussion started: 15 December 2025

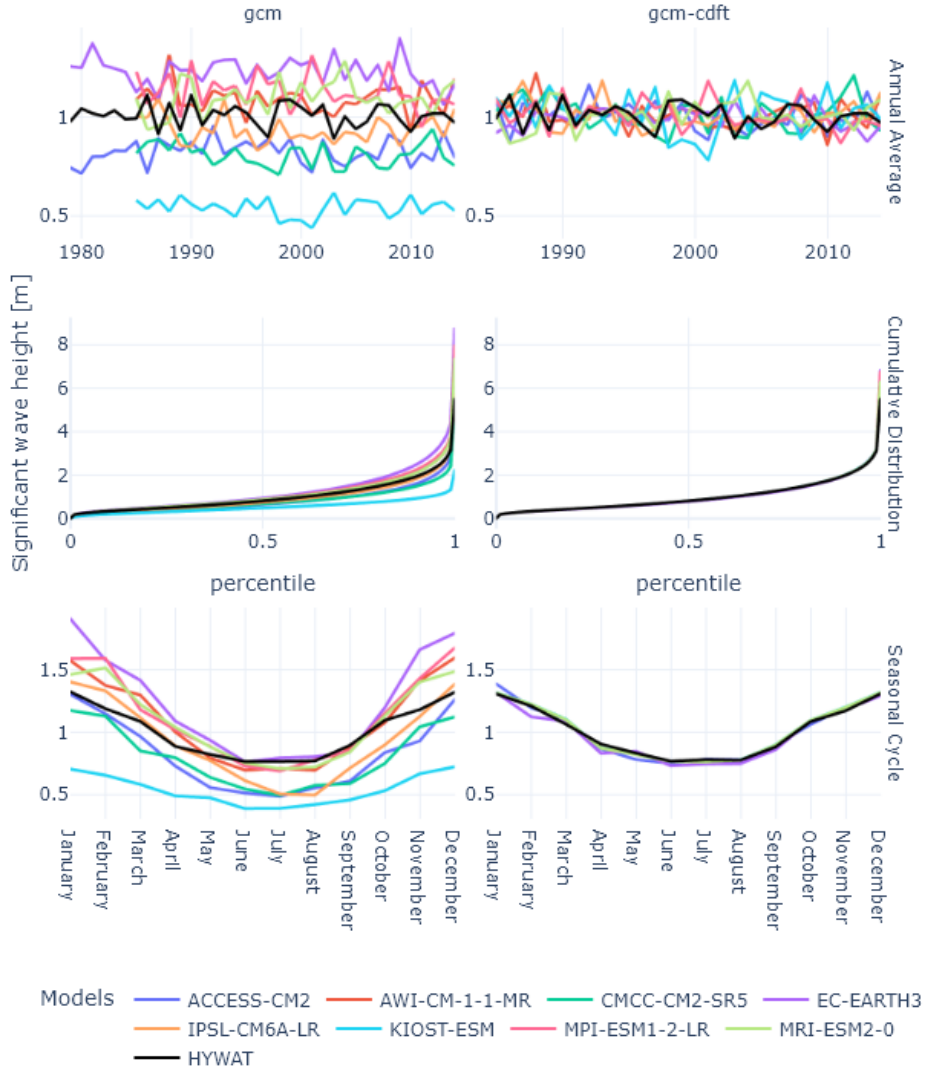

Figure 1. CDF-t validation over the Eastern Channel point for significant wave height. Climate models and reanalysis, respectively annual average, cumulative distribution and seasonal cycle from top to bottom. Before CDF-t (left) and after CDF-t (right).

along with a case-specific time criterion to separate events, by a Generalized Pareto Distribution (GPD). In a changing climate perspective, and since there are many parameters to tune by hand, the POT approach was not appropriate for our case.

In order to obtain a sufficient amount of data for fitting the GEV distribution, monthly maxima were used in this study. It implies that the seasonality has to be taken into account (e.g. (Reinert et al., 2021; Roustan et al., 2022; Cheynel et al., 2025)), which has been done using a non-parametric spline model for the parameters of the GEV. More precisely, the model writes:

https://doi.org/10.5194/wes-2025-266
Preprint. Discussion started: 15 December 2025

$$M_{\text{m,n}} \sim \text{GEV}(\mu = f_1(\text{m}), \sigma = f_2(\text{m}), \xi), \tag{3}$$

where m is the month of year n, and $M_{\text{m,n}}$ is the maximal value observed for this month and year. f_1 and f_2 are spline functions defined as a function of the month, assuming they are circular in m. Because estimating ξ is difficult (see Coles (2001)), it is assumed to be constant for all the months. It was also verified that the residuals from these models are independent and stationary (not shown here). Because the monthly maxima can be considered independent, we can compute the return level for any return period, by considering that the cumulative distribution function (CDF) of the annual maximum is the product of the monthly CDF (see (Youngman, 2022)):

$$\mathbb{P}(M \leq x) = \prod_{m=1}^{12} \mathbb{P}(M_m \leq x), \tag{4}$$

where M denotes the distribution of the annual maxima. By taking z_T such that $\mathbb{P}(M \leq z_T) = 1 - \frac{1}{T}$, we obtain the T-year return level, which is possible by numerical inversion of Equation 4. This approach also allows computing monthly return levels, which is important for the planning of operations, but will not be covered here because it is beyond the scope of this paper. More details can be found in (Raillard et al., in prep.).

The GEV model has been fitted for each variable, independently for each GCM, scenario, and time period when relevant, using the `{evgam}` R package (Youngman, 2022).

2.4 Confidence indices

In order to help the reader in interpreting the robustness of changes between two climatic periods, we have defined two indices: -1- the Significance Level ("SL"). It indicates the percentage of climate models that present a significant change in the sense of the Cramer Von Mises test. -2- the Agreement Level ("AL"). It indicates the percentage of models that agree on the sign of the change (increase or decrease). These indices are classified into five categories presented in the figure 2. The IPCC Sixth Assessment Report (AR6) for Europe (IPCC, 2022) also uses this kind of indices with a model congruence/consistency as a measure for the robustness and uncertainty of climate change signals. The changes are defined as robust if more than 66% of the ensemble members agree on the sign of change.

SL = Significance Level				
AL = Agreement Level				
VL	L	M	H	VH
[0;20%[	[20%;40%[	[40%;60%[	[60%;80%[	[80%;100%[

Figure 2. Confidence indices classification used in this study.

https://doi.org/10.5194/wes-2025-266
Preprint. Discussion started: 15 December 2025

eawe european academy of wind energy
Open Access WIND ENERGY SCIENCE DISCUSSIONS

3 Main results

To align with AR6, the baseline period of the study for mean conditions is 1995-2014. Two other future periods are defined to be studied under different scenarios: the medium-term period, from 2041 to 2060 and the long-term period from 2081 to 2100. Regarding changes in extreme conditions, 30-year periods are defined to make statistical calculations more robust. These periods are: baseline (1985-2014), mid-term future (2036-2065) and long-term future (2071-2100).

3.1 Changes in mean conditions

A general decrease is observed across all French maritime fronts in mean wind speed and significant wave height across all SSP scenarios. The trend is more pronounced along the Atlantic and Mediterranean coasts, especially in the long-term horizon (2081–2100). Water levels show a consistent increasing trend across all seafronts.

10 m Wind Speed. A general weakening trend in mean wind speed is observed across all French maritime fronts, particularly for the long-term period. This trend is more significant for the Atlantic coast. Under the SSP2-4.5 scenario, which is the scenario that has been chosen for the French Reference Trajectory for the Adaptation to Climate Change (TRACC)[4], the multi-model ensemble indicates (figure 3) a median decrease ranging from -0.4% to -2% for the mid-term horizon (around 2050) and -1.5% to -3.3% for the end of the century, relative to the baseline period (1995-2014). This is consistent with the findings of the AR6 (IPCC, 2022) and recent studies. Carvalho et al. (2021) show notable differences compared to CMIP5, with a general decline in wind resources. Jung and Schindler (2022) provide a recent literature synthesis, confirming the robustness of these downward trends for a range of scenarios. However, the spread among climate models remains substantial, with individual projections respectively ranging from –6% to +4% (from –10% to +4.5%) for the mid-term (long-term) horizon. Confidence in these changes is high to very high, especially under SSP3-7.0 and SSP5-8.5 scenarios for the Atlantic and Mediterranean coasts (SL and Al indicators above 85%). Seasonally, the most pronounced decreases occur during summer months, in agreement with CMIP6-based studies over the North Sea and Baltic regions (Hahmann et al., 2022).

Waves. For waves, only the SSP1-2.6 and SSP5-8.5 scenarios are available, and only for the long-term horizon (end of the century). The median significant wave height is projected to decrease under SSP1-2.6 (except for the eastern Mediterranean where climate models are in disagreement) and SSP5-8.5, with reductions between –2% and –6% under the second emission scenario (table 6). Model spread remains large (–11% to +3%), but confidence in the downward trend is very high for this scenario. This trend is less pronounced in the English Channel than on the other seafronts. Seasonal variations in significant wave height Hs show no clear evolution, and changes in peak wave period (Tp) are negligible (not shown here). These results are consistent with CMIP6-derived wave climate ensembles for European seas (Meucci et al., 2023). Lemos et al. (2021) and Bricheno and Wolf (2018) also identified a decrease in significant wave heights in the North Atlantic, supporting our observed results.

Water levels. Mean Sea Level (MSL) is projected to rise at all six representative points, with increases between +15 cm and +17 cm by 2100 (table 7), in agreement with IPCC AR6 regional projections (IPCC, 2022). Storm surges (negative or positive)

[4]https://www.ecologie.gouv.fr/sites/default/files/documents/document-reference-TRACC.pdf

https://doi.org/10.5194/wes-2025-266
Preprint. Discussion started: 15 December 2025

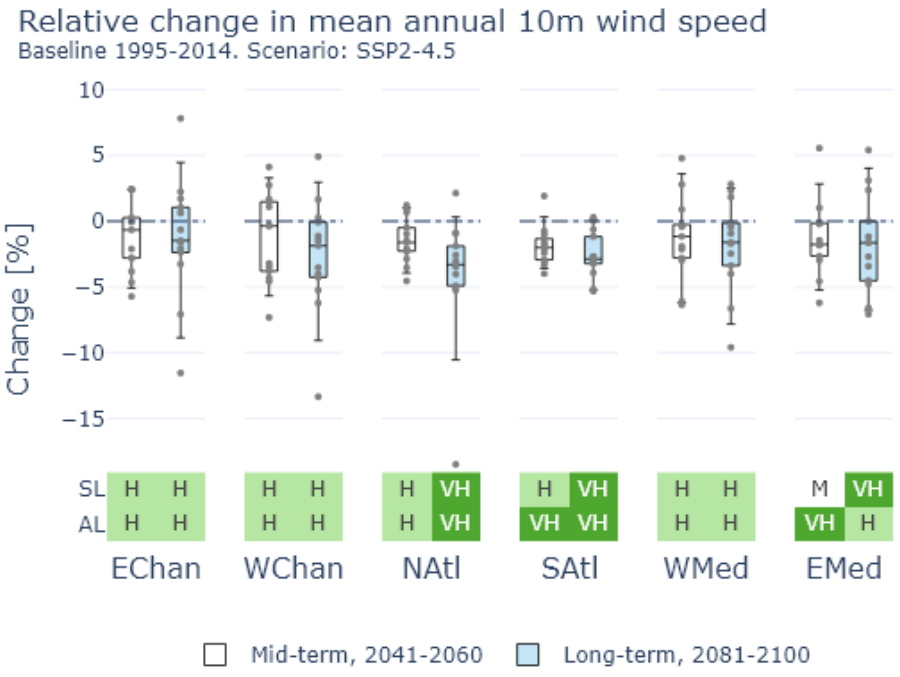

Figure 3. Relative change (in %) in annual mean 10 m wind speed at all representative points of French seafronts, under SSP2-4.5 scenario and relative to the baseline period (1995-2014). Confidence indices (bottom), Significance Level (SL) and Agreement Level (AL) are classified from Very Low (VL) to Very High (VH).

Table 6. Annual mean Hs changes at the 6 representative points, confidence intervals, significance level and agreement level under SSP1-2.6 and SSP5-8.5 scenarios.

Location	SSP1-2.6				SSP5-8.5			
	Median [%]	[p5 ; p95] [%]	SL [%]	AL [%]	Median [%]	[p5 ; p95] [%]	SL [%]	AL [%]
EChan (East Channel)	-3.7	[-6.7 ; -0.2]	62	87.5	-1.7	[-7.3 ; 2.9]	88	62.5
WChan (West Channel)	-2.7	[-4.8 ; 0.7]	75	75	-3.1	[-8.2 ; -0.3]	88	100
NAtl (North Atlantic)	-0.8	[-2.5 ; 1.2]	38	75	-4.2	[-8.0 ; -1.0]	88	100
SAtl (South Atlantic)	-1.5	[-4.2 ; 1.3]	50	75	-5.4	[-10.9 ; -1.6]	88	100
WMed (West Mediterranean)	-1.4	[-3.7 ; 2.8]	62	62.5	-5.7	[-7.8 ; -0.4]	88	100
EMed (East Mediterranean)	0.0	[-2.5 ; 2.4]	50	50	-4.4	[-8.5 ; -0.5]	88	87.5

show a rather downward trend (i.e. a decrease) in the future, always compared to the baseline period. However, these changes are very small (variations between 0 and -0.4 cm) and sometimes have equally low confidence indices, confirming the findings of regional sea level assessments for France (BRGM et al., 2018).

https://doi.org/10.5194/wes-2025-266
Preprint. Discussion started: 15 December 2025

eawe european academy of wind energy
Open Access WIND ENERGY SCIENCE DISCUSSIONS

Table 7. Absolute changes of mean sea levels (MSL) and surges (negative and positive) between the mid-term future period (2041–2060) and the baseline period (1995–2014), confidence intervals, significance level and agreement level.

Location	Component	Median [cm]	[p5 ; p95] [cm]	SL [%]	AL [%]
EChan (East Channel)	MSL	3.4	–	–	–
	Positive surge	-0.2	[-5.1 ; 2.4]	69	61.5
	Negative surge	-0.1	[-6.4 ; 2.0]	54	53.8
WChan (West Channel)	MSL	2.8	–	–	–
	Positive surge	-0.4	[-5.7 ; 3.3]	69	61.5
	Negative surge	-0.5	[-5.7 ; 3.4]	69	61.5
NAtl (North Atlantic)	MSL	1.9	–	–	–
	Positive surge	-1.6	[-3.9 ; 1.0]	62	76.9
	Negative surge	-0.5	[-4.3 ; 2.3]	54	69.2
SAtl (South Atlantic)	MSL	2.1	–	–	–
	Positive surge	-0.1	[-3.6 ; 0.3]	77	92.3
	Negative surge	-0.2	[-4.4 ; 2.0]	54	61.5
WMed (West Mediterranean)	MSL	3.0	–	–	–
	Positive surge	-0.2	[-6.2 ; 3.6]	69	76.9
	Negative surge	-0.2	[-6.2 ; 2.4]	62	69.2
EMed (East Mediterranean)	MSL	2.5	–	–	–
	Positive surge	-0.3	[-5.2 ; 2.8]	54	84.6
	Negative surge	-0.3	[-4.4 ; 2.1]	54	76.9

3.2 Changes in extreme conditions

Extreme significant wave heights tend to increase under future climate scenarios, particularly under SSP5-8.5. Wind speed extremes show less consistent patterns. Sea level extremes also show upward trends.

Extreme 10 m Wind Speed. No clear consensus emerges regarding the evolution of the extreme wind speed medians (figure 4). Under SSP5-8.5, a slight median increase is projected in the Channel (+2% to +5%) and on the Atlantic coast (+1% to +3%) for the end of the century (period 2071-2100), while there is a stagnation in the Mediterranean Sea. At the mid-term horizon (2036-2065), there is a slight median increase at the North Atlantic point (+3%) while there is a stagnation of the 50-year return values of 10 m wind speed in the Channel, and a decrease (-1% to -5%) at the other points (South Atlantic and Mediterranean). Model uncertainties are substantial, ranging from –15% to +15%. These findings align with recent European studies showing that climate change is already affecting the frequency of extreme wind events, with implications for offshore wind power availability (Rapella et al., 2023). Larsén et al. (2023), who use CMIP6 data to assess future extreme wind events, show an overall increase (<3%) in the extreme winds in the North Sea and the southern Baltic Sea, but a decrease (<5%) over the Scandinavian Peninsula and most of the Baltic Sea.

https://doi.org/10.5194/wes-2025-266
Preprint. Discussion started: 15 December 2025

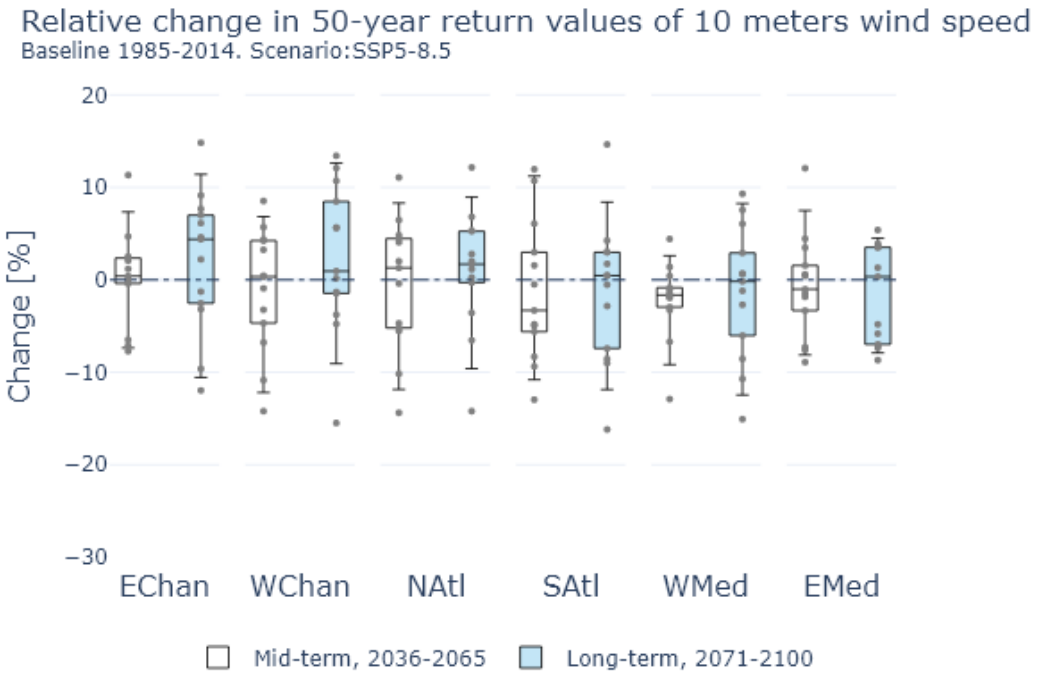

Figure 4. Relative change in 50-year return values of 10 m wind speed at representative locations, between SSP5-8.5 projections (mid-term: 2036-2065, long-term: 2071-2100) and the baseline period for extremes (1985-2014).

Extreme wave height. Extreme wave conditions are projected to intensify under future climate scenarios (table 8), particularly in the Mediterranean Sea under the SSP1-2.6 scenario, with a median increase of more than 15% (more than 2 m increase in the fifty-year Hs return value to the west of the Mediterranean coast. The opposite is true under the SSP5-8.5 scenario, with an increase of less than 10% in the Mediterranean Sea and more than 10% along the other seafronts. However, the model spread remains large, with an intermodel range of up to 13 m in the western Mediterranean (a possible change of more than 50%), reflecting a disparity between the models and likely owing to uncertainties in the representation of storm dynamics and wind-wave interactions, as mentioned in (Meucci et al., 2023; Susini et al., 2022). These findings are consistent with Bricheno and Wolf (2018) and Laugel et al. (2014), who compare dynamical and statistical downscaling methods for wave climate projections along the French coast, or Aarnes et al. (2017) in the Northeast Atlantic, and Charles et al. (2012) in the Bay of Biscay.

Extreme water levels. Extreme sea levels, represented by positive and negative storm surges, are expected to increase in magnitude (tables 9 and 10), with changes ranging from 3 cm to 28 cm (1 cm to 6 cm) for positive storm surges (negative storm surges). The strongest changes are observed in the English Channel and the weakest in the Mediterranean. These changes are of the same order as those projected for MSL (table 7). This reinforces the need to consider both mean and extreme water levels in offshore infrastructure design (IPCC, 2022; BRGM et al., 2018). This increase in extreme water levels is well documented by

https://doi.org/10.5194/wes-2025-266
Preprint. Discussion started: 15 December 2025

eawe european academy of wind energy
Open Access WIND ENERGY SCIENCE DISCUSSIONS

Table 8. Model mean 50-year return level values of significant wave height (RV50) and 95% confidence intervals (CI95) at representative locations, from the monthly maxima models: baseline period for extremes [1985-2014] and future period [2071-2100].

Location	Historical		SSP1-2.6		SSP5-8.5	
	RV50 [m]	CI95 [m]	RV50 [m]	CI95 [m]	RV50 [m]	CI95 [m]
East Channel (EChan)	5.95	[5.31 ; 6.59]	6.24	[4.78 ; 7.71]	6.58	[5.55 ; 7.61]
West Channel (WChan)	7.01	[6.21 ; 7.81]	7.49	[6.43 ; 8.55]	7.87	[6.45 ; 9.29]
North Atlantic (NAtl)	12.00	[10.94 ; 13.07]	12.93	[11.13 ; 14.73]	13.25	[11.05 ; 15.46]
South Atlantic (SAtl)	11.15	[9.97 ; 12.33]	12.25	[10.20 ; 14.30]	12.61	[10.92 ; 14.30]
West Mediterranean (WMed)	13.40	[8.99 ; 17.82]	15.74	[9.25 ; 22.24]	14.87	[8.85 ; 20.89]
East Mediterranean (EMed)	8.79	[7.14 ; 10.43]	9.71	[6.83 ; 12.59]	9.13	[6.41 ; 11.85]

Vousdoukas et al. (2017) and Muis et al. (2023), who provide global projections of storm surges using high-resolution CMIP6 models, reinforcing the importance of considering these hazards in offshore wind design.

Table 9. Model mean 50-year return level values of positive storm surges (RV50) and 95% confidence intervals (CI95) at representative locations, from monthly maxima models: baseline period for extremes [1985-2014] and future period [2031-2050].

Location	Historical		SSP5-8.5	
	RV50 [m]	CI95 [m]	RV50 [m]	CI95 [m]
East Channel (EChan)	1.50	[1.10 ; 1.89]	1.78	[1.28 ; 2.27]
West Channel (WChan)	1.23	[0.97 ; 1.48]	1.31	[1.04 ; 1.59]
North Atlantic (NAtl)	0.84	[0.73 ; 0.96]	0.93	[0.77 ; 1.10]
South Atlantic (SAtl)	0.78	[0.69 ; 0.87]	0.93	[0.56 ; 1.29]
West Mediterranean (WMed)	0.55	[0.51 ; 0.59]	0.60	[0.53 ; 0.66]
East Mediterranean (EMed)	0.51	[0.47 ; 0.56]	0.54	[0.46 ; 0.61]

4 Application to offshore wind

195 Following the approach recommended by recent climate impact assessments on wind energy systems (e.g., Pryor et al. (2020); Carvalho et al. (2021)), this section translates projected changes in atmospheric and oceanic conditions into operational and structural implications for offshore wind farms. We focus on two key dimensions: energy yield variability and evolving design constraints under CMIP6-based scenarios.

https://doi.org/10.5194/wes-2025-266
Preprint. Discussion started: 15 December 2025

eawe european academy of wind energy
Open Access WIND ENERGY SCIENCE DISCUSSIONS

Table 10. Model mean 50-year return level values of negative storm surges (RV50) and 95% confidence intervals (CI95) at representative locations, from monthly maxima model: baseline period for extremes [1985-2014] and future period [2031-2050]

Location	Historical		SSP5-8.5	
	RV50 [m]	CI95 [m]	RV50 [m]	CI95 [m]
East Channel (EChan)	-0.72	[-0.61 ; -0.83]	-0.75	[-0.60 ; -0.90]
West Channel (WChan)	-0.71	[-0.62 ; -0.80]	-0.77	[-0.58 ; -0.96]
North Atlantic (NAtl)	-0.45	[-0.42 ; -0.49]	-0.49	[-0.44 ; -0.55]
South Atlantic (SAtl)	-0.45	[-0.39 ; -0.51]	-0.49	[-0.45 ; -0.53]
West Mediterranean (WMed)	-0.39	[-0.36 ; -0.42]	-0.40	[-0.36 ; -0.44]
East Mediterranean (EMed)	-0.35	[-0.33 ; -0.37]	-0.37	[-0.34 ; -0.40]

4.1 Evolution of wind energy production

To assess the projected impact of climate change on offshore wind energy production, a standard 15 MW wind turbine model developed by NREL[5], with a hub height of 150 meters, is used. The downscaled wind speed at 10 m (see Section *Data and Methods*) is extrapolated to 150 m using a time-of-day and month-dependent vertical scaling coefficient. This coefficient is following the methodology developed by the Copernicus Climate Change Service for Energy (C3S Energy), which derived gridded α matrices (24 hours × 12 months) from 10 years of ERA5 hourly data at 10 m and 100 m[6].

The wind-to-power conversion is performed using the Python package `PyWake`[7], assuming a maximum power coefficient (C_p) of 0.49 and an ambient turbulence intensity (TI) of 7.9%, as characterized by Thiébaut and et al. (2024) using offshore Lidar measurements in the French Atlantic and Mediterranean zones. Intra- and inter-farm wake effects are not considered in this study.

Wind energy production is evaluated for two future periods—medium-term (2041–2060) and long-term (2081–2100)—relative to a historical baseline (1995–2014). Seasonal variations are also analyzed.

Table 11 presents the projected changes in annual energy production (AEP) at 150 m across the six representative offshore locations. A general decrease is observed across all French seafronts and emission scenarios, for both future horizons. Median changes range from –1% to –8%, with a wide uncertainty range due to inter-model variability (up to 15% between the 5th and 95th percentiles). Some models even project positive changes in AEP. Confidence levels (based on significance and model agreement) are generally high, except under the SSP1-2.6 scenario.

Seasonally, the most pronounced decreases are observed in summer and autumn under SSP3-7.0 and SSP5-8.5, with average reductions between –5% and –10%. These results are consistent with previous studies such as Barkanov et al. (2024), Carvalho et al. (2017), and Costoya et al. (2022), which also report seasonal declines in wind energy potential. However, unlike those

[5]https://nrel.github.io/turbine-models/2020ATB_NREL_Reference_15MW_240.html
[6]https://confluence.ecmwf.int/pages/viewpage.action?pageId=439598955
[7]https://topfarm.pages.windenergy.dtu.dk/PyWake/index.html

https://doi.org/10.5194/wes-2025-266
Preprint. Discussion started: 15 December 2025

eawe european academy of wind energy
Open Access WIND ENERGY SCIENCE DISCUSSIONS

studies, a significant increase in winter production is not observed here. This discrepancy may stem from differences in turbine characteristics, site selection, or the set of climate models used.

These findings agree with broader European assessments. Pryor et al. (2020) emphasize the sensitivity of wind power generation to climate-induced changes in wind regimes and the need for regional-scale evaluations. Carvalho et al. (2021) show that CMIP6 projections indicate a more pronounced decline in wind energy potential over Europe compared to CMIP5, particularly in southern and western regions. Jung and Schindler (2022) provide a comprehensive review of wind resource projections, highlighting the importance of turbine operating ranges—in our case, 4 m/s to 25 m/s.

Table 11. Projected changes in annual mean wind energy production at 150 m for the six representative offshore locations. Values are given for the median change, the 5th–95th percentile range, and the confidence indices: Significance Level (SL) and Agreement Level (AL).

Location	Scenario	2041–2060				2081–2100			
		Median (%)	[p5;p95]	SL (%)	AL (%)	Median (%)	[p5;p95]	SL (%)	AL (%)
EChan (East Channel)	SSP1-2.6	-4.1	[-13.0 ; 1.6]	85	85	-3.6	[-13.3 ; 2.3]	85	77
	SSP2-4.5	-1.9	[-6.1 ; 1.6]	62	77	-3.4	[-12.1 ; 3.3]	69	62
	SSP3-7.0	-0.9	[-7.7 ; 1.9]	54	69	-4.0	[-13.5 ; 0.1]	77	85
	SSP5-8.5	-2.4	[-5.5 ; 2.0]	77	69	-3.6	[-10.8 ; 0.8]	77	85
WChan (West Channel)	SSP1-2.6	-2.8	[-7.5 ; 3.7]	77	69	-1.8	[-7.8 ; 4.0]	54	77
	SSP2-4.5	-2.6	[-8.5 ; 2.8]	69	62	-4.8	[-12.8 ; 2.7]	77	85
	SSP3-7.0	-1.3	[-8.0 ; 3.6]	69	62	-2.5	[-12.3 ; 0.4]	62	85
	SSP5-8.5	-0.5	[-5.3 ; 3.2]	77	62	-3.9	[-10.2 ; 1.5]	77	85
NAtl (North Atlantic)	SSP1-2.6	-2.8	[-4.5 ; 2.9]	69	77	-1.7	[-5.3 ; 1.6]	31	62
	SSP2-4.5	-2.6	[-6.5 ; 0.3]	62	85	-5.91	[-7.8 ; -0.3]	75	92
	SSP3-7.0	-1.4	[-6.2 ; 1.5]	54	62	-4.7	[-9.8 ; -2.3]	92	100
	SSP5-8.5	-3.3	[-7.0 ; 0.6]	62	62	-6.3	[-10.9 ; -2.1]	100	100
SAtl (South Atlantic)	SSP1-2.6	-3.4	[-6.3 ; 1.7]	62	77	-1.6	[-6.0 ; 0.2]	46	85
	SSP2-4.5	-3.8	[-6.6 ; -0.2]	77	92	-5.3	[-8.2 ; -1.6]	77	100
	SSP3-7.0	-2.0	[-6.9 ; 2.1]	54	77	-5.7	[-11.6 ; -1.5]	92	92
	SSP5-8.5	-4.5	[-7.8 ; 0.5]	69	85	-7.8	[-13.0 ; -2.1]	92	100
WMed (West Mediterranean)	SSP1-2.6	-2.4	[-6.8 ; 0.9]	54	92	-1.3	[-8.0 ; 1.7]	46	77
	SSP2-4.5	-2.3	[-7.0 ; 2.5]	77	77	-1.8	[-8.2 ; 1.8]	77	77
	SSP3-7.0	-2.7	[-7.7 ; 1.3]	69	85	-3.7	[-9.1 ; -0.1]	92	92
	SSP5-8.5	-1.1	[-5.4 ; 0.4]	54	92	-6.0	[-13.4 ; -0.6]	92	100
EMed (East Mediterranean)	SSP1-2.6	-2.4	[-5.8 ; 2.3]	77	77	-1.6	[-5.3 ; 3.4]	85	69
	SSP2-4.5	-2.4	[-5.2 ; 2.7]	69	77	-2.7	[-6.9 ; 3.2]	92	69
	SSP3-7.0	-2.0	[-5.3 ; 1.2]	62	77	-4.0	[-8.9 ; 2.9]	92	77
	SSP5-8.5	-2.6	[-6.1 ; 3.3]	85	77	-6.0	[-14.0 ; 1.6]	85	85

https://doi.org/10.5194/wes-2025-266
Preprint. Discussion started: 15 December 2025

eawe european academy of wind energy
Open Access WIND ENERGY SCIENCE DISCUSSIONS

4.2 Evolution of design conditions

To assess how design conditions for offshore wind farms may evolve under climate change, two complementary aspects were investigated within the 2C NOW project. The first concerns the impact of changing metocean conditions on turbine fatigue design, evaluated through variations in Damage Equivalent Loads (DEL) across multiple climate scenarios. The second addresses the morphological evolution of a cable landfall site, based on a methodology combining current industry practices with state-of-the-art approaches for modeling future beach dynamics (Cadiou and Yates, 2025).

4.2.1 Fatigue design of offshore wind turbines

The analysis focuses on four offshore wind farm sites in France—Saint-Nazaire, Saint-Brieuc, Fécamp, and Courseulles-sur-Mer—using five wave climate models previously described. These models, corrected through the CDF-t statistical downscaling method under SSP1-2.6 and SSP5-8.5 scenarios, were selected because they are the only ones common to the wind climate model ensemble. The methodology follows a structured approach (illustrated in figure 5):

1. Environmental Data Processing: Historical and future climate data (wind speed, wave height, and wave period) are collected and processed to define a range of environmental conditions for simulations.

2. Aeroelastic Simulations: A database of fatigue operating simulations, covering the range of environmental conditions defined in the first step, is generated using the open-source OpenFAST software and the IEA 10 MW offshore wind turbine model with a monopile foundation. The simulations are then post-processed to obtain a DEL for each simulation.

3. Interpolation & Analysis: DELs are interpolated from the DEL database for different climate models and scenarios, based on the wind speed, wave height, and wave period values. Trends in fatigue loads are analyzed.

Particular attention is given to the two tower base moments along the horizontal axis (Mx and My), as these loading directions typically drive the structural design (Mozafari et al., 2024). Results indicate a general trend of decreasing Mx and My tower base DEL across most scenarios and sites (figure 6), compared to historical levels, suggesting that offshore wind turbines could experience lower fatigue loads in the future (of the order of -1% to -2% on average). This trend, if confirmed, could extend the operational lifespan of offshore wind farms, partially offsetting potential drawbacks from more extreme weather conditions. However, the estimated changes show high variability between climate models and different sites, with some models showing load increases. This highlights the need for careful consideration of uncertainties.

4.2.2 Evolution of a landing site

Morphological changes in the cable landfall zone may cause two different effects on offshore submarine cables. First, with erosion, cables may become uncovered and experience free spanning, where they are exposed to mechanical forces and potential failure. Second, with accretion, they may be subject to excessive burial, which can cause overheating, reduced electrical transmission performance, and even failure. Building on the bibliographic study of Cadiou and Yates (2025) identifying the current

https://doi.org/10.5194/wes-2025-266
Preprint. Discussion started: 15 December 2025

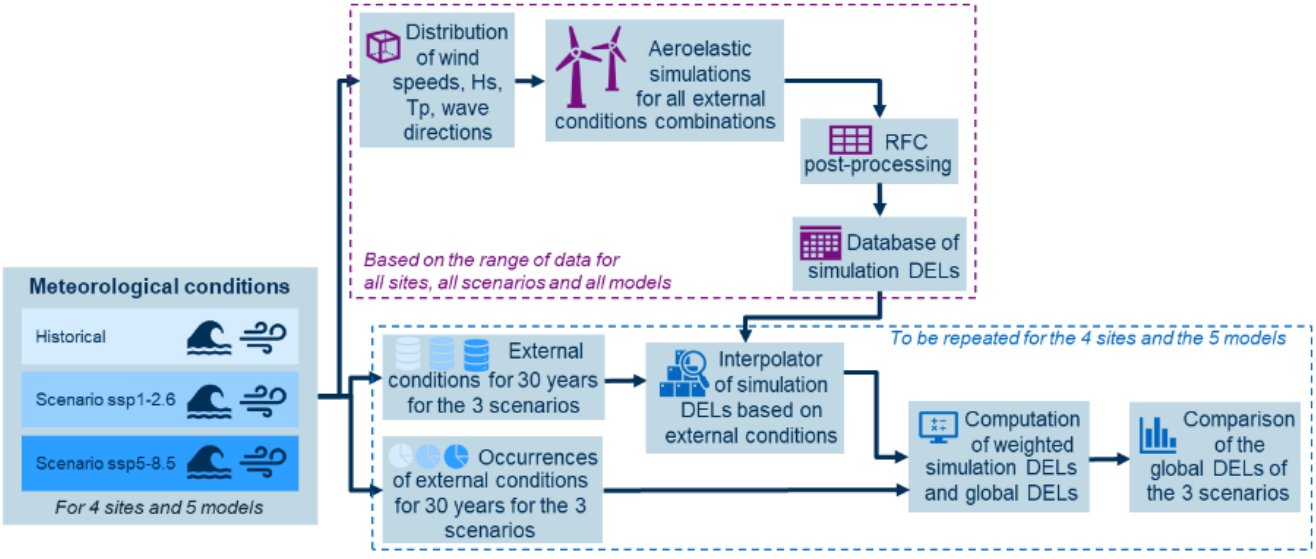

Figure 5. General methodology for fatigue design assessment.

state of the art in the evaluation of the projections of morphological changes at multidecadal timescales, a methodology for evaluating the impacts of climate change on cable landfall sites is proposed here. This methodology consists of four phases: (1) collecting all relevant hydrodynamic and morphological data (observations and simulation results) at the selected study site, (2) selecting the appropriate future wave condition and water levels scenarios, (3) modeling beach morphological changes using empirical and numerical models at short-term, event-based and medium to long-term timescales using two different modeling approaches, and (4) combining the modeling results with estimates of the associated uncertainties to define the threat line. This threat line can then be used in conjunction with a study of the thermal resistance of the cables, including the local sediment properties and water temperature, to define the cable burial depth. This methodology was applied at Porsmilin Beach (Brittany, France), a site which is not a potential cable landfall site but has been studied for over fifteen years, with sufficient hydrodynamic and morphological observations and simulation outputs to complete a thorough study of the beach morphological evolution. This is an essential element in any study of a potential cable landfall site, which enables characterizing its historical morphological evolution and calibrating the selected morphological evolution models. To estimate the maximum vertical variations in nearshore sand levels, it is essential to consider both the long-term beach response to sea-level rise and wave climate, as well as the short-term changes induced by extreme events. In this study, numerical projections of beach morphology were complemented by two modeling approaches: a process-based model to capture storm-driven, short-term evolution, and a reduced-complexity model to assess long-term trends. Only two of the eight wave climate models (ACCESS-CM2 and EC-Earth3) are used to investigate morphodynamics, as they are the only ones providing continuous data from the baseline period through 2100.

Short-term, storm-based morphological evolution

https://doi.org/10.5194/wes-2025-266
Preprint. Discussion started: 15 December 2025

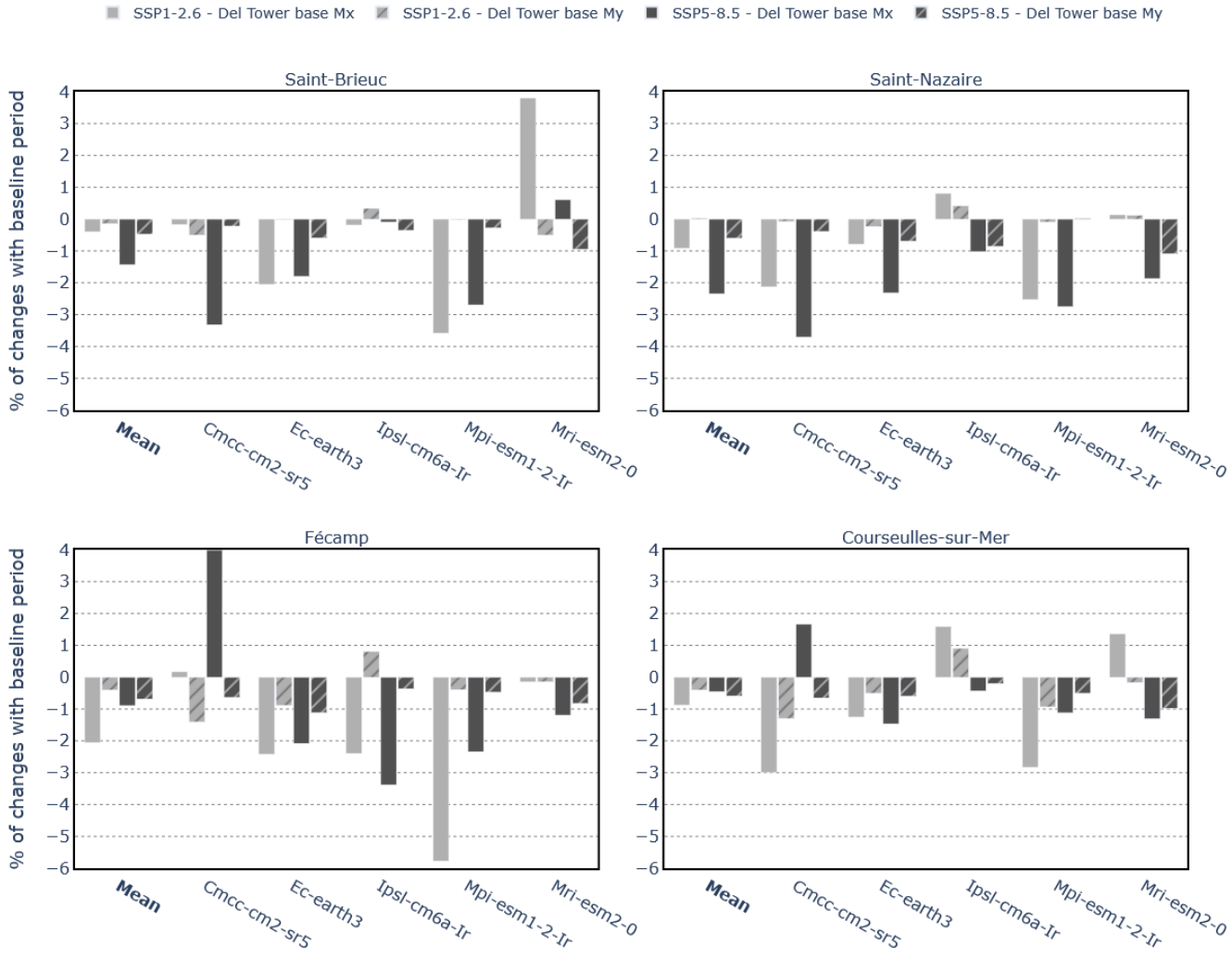

Figure 6. Comparison of tower base Mx and My DEL relative difference (in %) with historical values for all sites, models and scenarios.

To model the short-term morphological evolution, the XBeach model (Roelvink et al., 2009) was selected. This open-source model solves coupled 2D horizontal equations for wave propagation, flow, sediment transport and bottom changes, for varying wave conditions. In the present case, the longshore sediment transport can be considered as negligible at Porsmilin beach. Therefore, the 1D (cross-shore profile) resolution method is used in this study. This model is used to simulate the maximum expected changes in sand levels during extreme events defined as the wave conditions with a 50-year return period. To evaluate the impacts of climate change on morphological evolution, a reference simulation is run for an event with a 50-year return period based on historical data, and then each future 50-year return period event simulation is compared to this historical event.

https://doi.org/10.5194/wes-2025-266
Preprint. Discussion started: 15 December 2025

eawe european academy of wind energy
Open Access WIND ENERGY SCIENCE DISCUSSIONS

To determine the optimal burial depth of the cable, the maximum changes in sand level are evaluated along the beach profile, identifying the maximum erosion and accretion levels.

Table 12. Maximum input wave conditions extracted from the two wave climate datasets (ACCESS-CM2; EC-Earth3) and corresponding maximum accretions and erosions estimated by the XBeach model compared to the pre-storm profile, including a negative and positive storm surge (only under SSP5-8.5).

Wave climate datasets	**ACCESS-CM2**		**EC-Earth3**	
	Hs (m)	Tp (s)	Hs (m)	Tp (s)
Extreme values (50y)				
Historical	5.72	20.30	5.42	16.26
SSP1-2.6	4.41	20.45	5.24	18.00
SSP5-8.5	4.50	16.76	5.03	18.86
Maximum accretion (m)				
Historical period	1.79		1.39	
SSP1-2.6	1.62		1.41	
SSP5-8.5 (no surge)	1.32		1.26	
SSP5-8.5 with negative surge	1.68		1.74	
SSP5-8.5 with positive surge	2.08		1.89	
Maximum erosion (m)				
Historical period	-0.96		-1.26	
SSP1-2.6	-0.85		-1.13	
SSP5-8.5 (no surge)	-1.2		-1.32	
SSP5-8.5 with negative surge	-1.21		-1.34	
SSP5-8.5 with positive surge	-3.67		-4.3	

When considering the climate change scenario SSP1-2.6, the only difference in the data extracted from the ACCESS-CM2 wave climate model compared to the historical data is a reduction of the significant wave height 50-year extreme value by 1.3 m, while the peak wave period does not change (Table 12). This naturally results in a decrease in wave energy leading to a decrease in the associated currents and sediment transport (less accretion and erosion). For the EC-Earth3 model, the 50-year peak wave period (18 s) increases by almost 2 s relative to the historical period, and the significant wave height decreases by 0.2 m. This decrease in Hs causes a slight decrease in the maximum erosion reaching -1.13 m (compared to -1.26 m when considering the historical data). The maximum accretion is however not significantly impacted and remains at a similar value of 1.41 m (compared to 1.39 m considering the historical data). When considering scenario SSP5-8.5 compared to the historical data, the extreme wave conditions estimated using the ACCESS-CM2 model experience an important decrease in both significant wave height and peak period with respectively Hs = 4.5 m (compared to 5.72 m) and Tp = 16.76 s (compared to 20.30 s). Using these reduced parameters, the estimated accretion is also highly reduced to 1.32 m while the erosion is however increased reaching

https://doi.org/10.5194/wes-2025-266
Preprint. Discussion started: 15 December 2025

eawe european academy of wind energy
Open Access WIND ENERGY SCIENCE DISCUSSIONS

a maximum of -1.20 m. Using the EC-Earth3 model, the significant wave height and peak period are respectively set to 5.03 m (compared to 5.42 m) and 18.86 s (compared to 16.26 s). Despite these changes, the accretion and erosion are not significantly different from the historical data with respective estimation of 1.26 m and -1.32 m. To understand the influence of negative and positive storm surges on maximum accretion and erosion estimations, the same wave conditions from the ACCESS-CM2 and EC-Earth3 models were applied, considering a decrease of 1.63 m in water level for the negative surge and an increase of 2.2 m for the positive surge. Combined with waves, changes in water level naturally induce shifts in the position of the foreshore area, leading to an offshore shift of the sandbar and erosion area when the water level decreases, and a landward shift when the water level increases. For both positive and negative surge, and both climate models, the maximum accretion increases while the wave conditions remain the same. This increase could naturally be explained by the change in x position and the change in pre-storm seabed level. For the maximum erosion however, the results are similar when considering the negative surge, indicating a similar impact of the wave conditions despite the change in water level.

Long-term morphological evolution

The long-term morphological evolution is explored using a simpler, more computationally efficient reduced-complexity (or hybrid) model, combining an equilibrim-based shoreline model (Lemos et al., 2018) and the Bruun Rule (Bruun, 1962). This model is an extended version of the cross-shore model integrated in CoSMoS-COAST, , which has been tested and validated across the western coast of the United States (Vitousek et al., 2017). Lemos et al. (2018) adapted the application of the model to incorporate the effets of the tide level, which is important on meso and macrotidal beaches, such as those in France.

Figure 7 shows projections of the future profile position for the 3 sea-level rise projections (SSP1-2.6, SSP5-8.5 and the Permanent Service for Mean Sea Level, PSMSL, from Brest tide gauge data extrapolation) presented here in 2050 and 2100 by applying the Bruun rule. Notice that by 2050 (Figure 7a), the shoreline recedes, but the associated vertical translation of the profile causes very little change along the profile given the rather constant slope. By 2100 (Figure 7b), the shoreline recession is more significant, and the changes are more noticeable farther offshore than in 2050. Data are not available shoreward of beach profile measurements (stopping at x = 0 m), thus all changes in this zone cannot be estimated without additional information.

5 Conclusions

This study, conducted within the framework of the 2C NOW project, provides a comprehensive assessment of the potential impacts of climate change on offshore wind energy development along French coasts. By combining climate projections, statistical downscaling techniques, and targeted applications to wind energy production, turbine fatigue, and coastal morphodynamics, we offer a multi-faceted perspective on future challenges and opportunities for the offshore wind sector. Our results highlight a general decline in mean wind speed and wave height across all continental French seafronts and emission scenarios, with more pronounced changes expected by the end of the century. While these trends may reduce energy yield and increase the Levelized Cost of Energy (LCOE), they are partially offset by a projected decrease in fatigue loads on turbine structures. However, they are also accompanied by uncertainties greater than the trends themselves. Extreme events—particularly significant wave heights and storm surges—are expected to intensify, reinforcing the need for robust design standards and adaptive plan-

https://doi.org/10.5194/wes-2025-266
Preprint. Discussion started: 15 December 2025

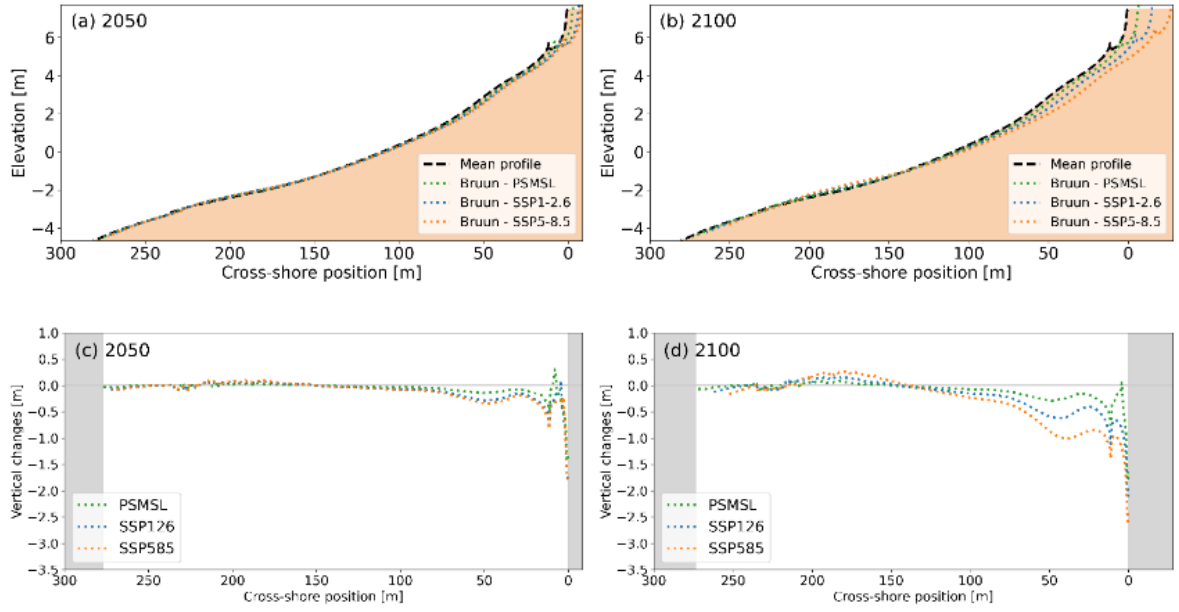

Figure 7. Beach profile projections (top) and the corresponding changes (bottom) in sediment layer thickness in (a,c) 2050 and (b,d) 2100 are estimated by applying the Bruun rule for three different SLR projections: PSMSL (green), SSP1-2.6 (blue), and SSP5-8.5 (orange), where the gray shading indicates zones where the profiles do not overlap.

ning. Although mean wind speeds and wave heights are projected to decline, our results indicate an intensification of extreme wave events. This apparent paradox can be explained by changes in variability: a shift in the mean combined with increased variance can lead to more frequent or more intense extremes, even in the opposite direction of the mean trend (see e.g. Kodra and Ganguly (2014)). Such behavior reflects the non-linear response of storm-driven processes to climate forcing. Physically, this may be linked to changes in storm characteristics, including their spatial distribution, trajectories, and translation speeds, which influence wave generation and propagation. Further investigation of these dynamics at regional scale would be necessary to confirm the mechanisms underlying these projected extremes. The morphodynamic analysis of a representative cable landfall site demonstrates the importance of integrating shoreline evolution into infrastructure planning, especially under scenarios of sea level rise and changing storm regimes. The proposed methodology, combining empirical and numerical models, offers a replicable framework for future site assessments. Overall, this work underscores the necessity of incorporating climate resilience into offshore wind development strategies. It also reveals key areas for future research, including the integration of multivariate and non-stationary extreme value models, the use of AI-enhanced downscaling techniques, and the consideration of full wind farm effects in energy yield assessments. As France and Europe accelerate their offshore wind deployment, such forward-looking analyses will be essential to ensure the long-term sustainability and reliability of this critical energy source.

https://doi.org/10.5194/wes-2025-266
Preprint. Discussion started: 15 December 2025

eawe european academy of wind energy
Open Access WIND ENERGY SCIENCE DISCUSSIONS

6 Limitations

Three main categories of limitations are identified: -1- Climate datasets (wind, waves, and water levels), which present limitations in terms of spatial and temporal resolution. The datasets used during the project are global datasets (IPCC's CMIP6). They have been statistically downscaled at the locations of interest, both temporally (from daily resolution to hourly resolution) and spatially (from the resolution of GCMs to those of reanalyses). -2- Mathematical methods, with statistical downscaling (here the CDF-t method was used), performed in univariate mode and not necessarily adapted to extreme events, and extreme analyses, which should be addressed in the future in multivariate and non-stationary mode. These mathematical methods could particularly benefit from recent advances in the use of AI (Richards and Huser, 2022; Allouche et al., 2024; Pasche and Engelke, 2024) and Deep Learning (Velthoen et al., 2023; Gnecco et al., 2024). -3- Offshore wind applications, primarily wind energy production calculations, which were limited in the 2C NOW project to a single turbine type and did not take into account the wake effects that occur in offshore wind farms; turbine fatigue and morphodynamic calculations in the landfall zone, which suffered from numerous assumptions due to very long calculation times and could also benefit from advances using AI to combine short and long-term simulations. All calculations performed during the project were based on climate datasets, the results of which may differ, and the precise estimation of uncertainties appears to be a key parameter in future studies.

Author contributions. YK led the project, coordinated all tasks, and wrote the majority of the manuscript, integrating contributions from all co-authors. BO was responsible for the analysis and writing of the wind and energy production section, with support from AP and TC. NR led the work on waves, water levels, extreme events, and design conditions, assisted by CP and TC. MY and MP contributed to the applications related to design, including fatigue analysis and coastal morphodynamics. LD acted as scientific advisor and provided expert review and guidance throughout the manuscript preparation.

Competing interests. The authors declare that they have no known competing financial interests or personal relationships that could have appeared to influence the work reported in this paper.

Acknowledgements. This work is performed within the Joint Industrial R&D Project 2C NOW, which receives funding from France Energies Marines and its members and partners, as well as French State funding, managed by the National Research Agency under the France 2030 investment plan (grant no. ANR-10-IEED-0006-34).

https://doi.org/10.5194/wes-2025-266
Preprint. Discussion started: 15 December 2025

eawe european academy of wind energy
Open Access WIND ENERGY SCIENCE DISCUSSIONS

References

Aarnes, O., Reistad, M., Breivik, , Bitner-Gregersen, E., Eide, L., Gramstad, O., Magnusson, A., Natvig, B., and Vanem, E.: Projected changes in significant wave height toward the end of the 21st century: Northeast Atlantic, Journal of Geophysical Research: Oceans, 122, 3394–3403, 2017.

Allouche, M., Girard, S., and Gobet, E.: Estimation of extreme quantiles from heavy-tailed distributions with neural networks, Statistics and Computing, forthcoming, 2024.

Barkanov, E., Penalba, M., Martinez, A., Martinez-Perurena, A., Zarketa-Astigarraga, A., and Iglesias, G.: Evolution of the European offshore renewable energy resource under multiple climate change scenarios and forecasting horizons via CMIP6, Energy Conversion and Management, 301, 118 058, https://doi.org/10.1016/j.enconman.2024.118058, 2024.

BRGM, Ocean, M., and LEGOS/OMP: Vagues et hausse du niveau de la mer : de nouveaux résultats de recherche, urlhttps://www.brgm.fr/fr/actualite/actualite/vagues-hausse-niveau-mer-nouveaux-resultats-recherche, consulté en septembre 2025, 2018.

Bricheno, L. and Wolf, J.: Future Wave Conditions of Europe, in Response to High-End Climate Change Scenarios, Journal of Geophysical Research: Oceans, 123, 8762–8791, https://doi.org/10.1029/2018JC013866, 2018.

Bruun, P.: Sea-level rise as a cause of shoreline erosion, Journal of the Waterways and Harbours Division, 88, 117–130, 1962.

Cadiou, O. and Yates, M.: Coastal evolution due to climate change and the impact on cables in the landfall zone, Technical report, France Énergies Marines, Ifremer, Innosea, Shell, Shom, Skyborn Renewables, RTE, https://www.france-energies-marines.org/wp-content/uploads/2025/04/2CNOW-Coastal-evolution-climate-change-final.pdf, 2C NOW project, 29 pages, 2025.

Carvalho, D., Rocha, A., Gómez-Gesteira, M., and Silva Santos, C.: Potential impacts of climate change on European wind energy resource under the CMIP5 future climate projections, Renewable Energy, 101, 29–40, https://doi.org/10.1016/j.renene.2016.08.036, 2017.

Carvalho, D., Rocha, A., Costoya, X., de Castro, M., and Gómez-Gesteira, M.: Wind energy resource over Europe under CMIP6 future climate projections: What changes from CMIP5 to CMIP6, Renewable and Sustainable Energy Reviews, 151, 111 594, https://doi.org/10.1016/j.rser.2021.111594, 2021.

Charles, E., Idier, D., Delecluse, P., Déqué, M., and G., L.: Climate change impact on waves in the Bay of Biscay, France, Ocean Dynamics, 62, 831–848, https://doi.org/10.1007/s10236-012-0534-8, 2012.

Cheynel, J., Pineau-Guillou, L., Lazure, P., Marcos, M., and Raillard, N.: Regional changes in extreme storm surges revealed by tide gauge analysis, Ocean Dynamics, 75, 29 (11p.), https://doi.org/10.1007/s10236-025-01675-6, 2025.

Coles, S.: An Introduction to Statistical Modeling of Extreme Values, Springer London, ISBN 9781447136750, https://doi.org/10.1007/978-1-4471-3675-0, 2001.

Costoya, X., deCastro, M., Carvalho, D., Arguilé-Pérez, B., and Gómez-Gesteira, M.: Combining offshore wind and solar photovoltaic energy to stabilize energy supply under climate change scenarios: A case study on the western Iberian Peninsula, Renewable and Sustainable Energy Reviews, 157, 112 037, https://doi.org/10.1016/j.rser.2021.112037, 2022.

European Commission: European Green Deal and REPowerEU, available at https://ec.europa.eu, 2020.

European Parliament: Offshore wind energy in Europe, briefing document, Ref. 659313, Available at https://www.europarl.europa.eu, 2020.

Gnecco, N., Terefe, E. M., and Engelke, S.: Extremal random forests, Journal of the American Statistical Association, forthcoming, 2024.

Hahmann, A. N., García-Santiago, O., and Peña, A.: Current and future wind energy resources in the North Sea according to CMIP6, Wind Energy Science, 7, 2373–2392, https://doi.org/10.5194/wes-7-2373-2022, 2022.

https://doi.org/10.5194/wes-2025-266
Preprint. Discussion started: 15 December 2025

Ibarra-Berastegui, G., Sáenz, J., Ulazia, A., González-Rojí, and Esnaola, G.: CMIP6 projections of wave climate change in the Mediterranean sea by the end of the twenty-first century, Ocean Engineering, 335, 121 704, https://doi.org/10.1016/j.oceaneng.2025.121704, 2025.

IPCC: Climate Change 2022: Impacts, Adaptation and Vulnerability, chap. Chapter 13: Europe, Cambridge University Press, https://www.ipcc.ch/report/ar6/wg2/chapter/chapter-13/, 2022.

Jung, C. and Schindler, D.: A review of recent studies on wind resource projections under climate change, Renewable and Sustainable Energy Reviews, 165, 112 596, https://doi.org/10.1016/j.rser.2022.112596, 2022.

Kodra, E. and Ganguly, A. R.: Asymmetry of projected increases in extreme temperature distributions, Scientific Reports, 4, 5884, https://doi.org/10.1038/srep05884, 2014.

Larsén, X., Imberger, M., Hannesdóttir, , and Hahmann, A.: The Impact of Climate Change on Extreme Winds over Northern Europe According to CMIP6, Wind Energy Science Discussions, https://doi.org/10.5194/wes-2022-102, 2023.

Laugel, A., Menéndez, M., Benoit, M., Mattarolo, G., and Méndez, F.: Wave climate projections along the French coastline: Dynamical versus statistical downscaling methods, Ocean Modelling, 84, 35–50, 2014.

Le Cozannet, G. and Cazenave, A.: Adaptation to sea level rise in France, Rendiconti Lincei. Scienze Fisiche e Naturali, 35, 1–18, https://doi.org/10.1007/s12210-024-01225-0, 2024.

Lemos, C., Floc'h, F., Yates, M., Le Dantec, N., Marieu, V., Hamon, K., Cuq, V., Suanez, S., and Delacourt, C.: Equilibrium modeling of the beach profile on a macrotidal embayed low tide terrace beach, Ocean Dynamics, 68, https://doi.org/10.1007/s10236-018-1185-1, 2018.

Lemos, G., Menéndez, M., Semedo, A., Miranda, P., and Hemer, M.: On the decreases in North Atlantic significant wave heights from climate projections, Climate Dynamics, 57, 2301–2324, https://doi.org/10.1007/s00382-021-05807-8, 2021.

Meucci, A., Young, I. R., Hemer, M., Trenham, C., and Watterson, I. G.: 140 Years of Global Ocean Wind-Wave Climate Derived from CMIP6 ACCESS-CM2 and EC-Earth3 GCMs: Global Trends, Regional Changes, and Future Projections, Journal of Climate, 36, 1605–1631, https://doi.org/10.1175/JCLI-D-21-0929.1, publisher: American Meteorological Society Section: Journal of Climate.

Meucci, A., Young, I., Hemer, M., and Trenham, C.: 140 Years of Global Ocean Wind-wave Climate Derived from CMIP6 ACCESS-CM2 and EC-Earth3 GCMs, Journal of Climate, pp. 1–56, https://doi.org/10.1175/JCLI-D-21-0929.1, 2023.

Michelangeli, P.-A., Vrac, M., and Loukos, H.: Probabilistic downscaling approaches: Application to wind cumulative distribution functions, Geophysical Research Letters, 36, https://doi.org/10.1029/2009GL038401, 2009.

Mozafari, S., Veers, P., Rinker, J., and Dykes, K.: Sensitivity of fatigue reliability in wind turbines: effects of design turbulence and the Wöhler exponent, Wind Energy Science, 9, 799–820, https://doi.org/10.5194/wes-9-799-2024, 2024.

Muis, S., Aerts, J., Antolínez, J., Dullaart, J., Duong, T., Erikson, L., Haarsma, R., Irazoqui Apecechea, M., Mengel, M., Le Bars, D., O'Neill, A., Ranasinghe, R., Roberts, M., Verlaan, M., Ward, P., and Yan, K.: Global Projections of Storm Surges Using High-Resolution CMIP6 Climate Models, Earth's Future, 11, 1–17, https://doi.org/10.1029/2023EF003479, 2023.

Pasche, O. C. and Engelke, S.: Neural networks for extreme quantile regression with an application to forecasting of flood risk, Annals of Applied Statistics, forthcoming, 2024.

Patra, A., Oueslati, B., Chevallier, T., Renaud, P., Kervella, Y., and Dubus, L.: Evaluation of ERA5, COSMO-REA6 and CERRA in simulating wind speed along the French coastline for wind energy applications, Advances in Science and Research, 22, 69–85, https://doi.org/10.5194/asr-22-69-2025, 2025.

Pryor, S., Barthelmie, R., and Bukovsky, M.: Climate change impacts on wind power generation, Nature Reviews Earth Environment, 1, 627–643, https://doi.org/10.1038/s43017-020-0101-7, 2020.

https://doi.org/10.5194/wes-2025-266
Preprint. Discussion started: 15 December 2025

Raillard, N., Poppeschi, C., Chevallier, T., and Kervella, Y.: Non-stationary GEV models for estimating design sea-states in a changing climate. Applications to offshore wind farms along the French coasts., in prep.

Rapella, L., Faranda, D., Gaetani, M., Drobinski, P., and Ginesta, M.: Climate change on extreme winds already affects off-shore wind power availability in Europe, Environmental Research Letters, 18, 034 040, https://doi.org/10.1088/1748-9326/acbdb2, 2023.

Reinert, M., Pineau-Guillou, L., Raillard, N., and Chapron, B.: Seasonal Shift in Storm Surges at Brest Revealed by Extreme Value Analysis, Journal of Geophysical Research: Oceans, 126, https://doi.org/10.1029/2021jc017794, 2021.

Richards, J. and Huser, R.: Regression modelling of spatiotemporal extreme U.S. wildfires via partially-interpretable neural networks, arXiv preprint arXiv:2208.07581, https://arxiv.org/abs/2208.07581, 2022.

Roelvink, D., Reniers, A., van Dongeren, A., van Thiel de Vries, J., McCall, R., and Lescinski, J.: Modelling storm impacts on beaches, dunes and barrier islands, Coastal Engineering, 56, 1133–1152, https://doi.org/10.1016/j.coastaleng.2009.08.006, 2009.

Roustan, J.-B., Pineau-Guillou, L., Chapron, B., Raillard, N., and Reinert, M.: Shift of the storm surge season in Europe due to climate variability, Scientific Reports, 12, https://doi.org/10.1038/s41598-022-12356-5, 2022.

Susini, S., Menendez, M., Eguia, P., and Blanco, J. M.: Climate Change Impact on the Offshore Wind Energy Over the North Sea and the Irish Sea, Frontiers in Energy Research, 10, https://doi.org/10.3389/fenrg.2022.881146, 2022.

Thiébaut, M. and et al.: Characterization of offshore turbulence intensity using Lidar measurements in the French maritime zones, Wind Energy Research, X, 100 002, https://doi.org/10.1016/j.weer.2024.100002, 2024.

Velthoen, J., Dombry, C., Cai, J.-J., and Engelke, S.: Gradient boosting for extreme quantile regression, Extremes, 26, 639–667, https://doi.org/10.1007/s10687-023-00473-x, 2023.

Vitousek, S., Barnard, P. L., Limber, P., Erikson, L., and Cole, B.: A model integrating longshore and cross-shore processes for predicting long-term shoreline response to climate change, Journal of Geophysical Research: Earth Surface, 122, 782–806, https://doi.org/10.1002/2016JF004065, 2017.

Vousdoukas, M., Feyen, L., Mentaschi, L., Voukouvalas, E., and Verlaan, M.: Extreme sea levels on the rise along Europe's coasts, Earth's Future, 5, 304–323, https://doi.org/10.1002/2016EF000505, 2017.

Wu, J., Zha, J., Zhao, D., and Yang, Q.: Changes in terrestrial near-surface wind speed and their possible causes: an overview, Climate Dynamics, 51, 2039–2078, https://doi.org/10.1007/s00382-017-3997-y, 2018.

Youngman, B. D.: evgam: An R Package for Generalized Additive Extreme Value Models, Journal of Statistical Software, 103, 1–26, https://doi.org/10.18637/jss.v103.i03, 2022.

Zeng, Z., Ziegler, A. D., Searchinger, T., Yang, L., Chen, A., Ju, K., Piao, S., Li, L. Z. X., Ciais, P., Chen, D., Liu, J., Azorin-Molina, C., Chappell, A., Medvigy, D., and Wood, E. F.: A reversal in global terrestrial stilling and its implications for wind energy production, Nature Climate Change, 9, 979–985, https://doi.org/10.1038/s41558-019-0622-6, 2019.